MASTER

CONF-8606135--1

Los Alamos National Laboratory is operated by the University of California for the United States Department of Energy under contract W-7405-ENG-36

RECEIVED
JUL 07 1986

TITLE POTPOURRI OF LOS ALAMOS NATIONAL LABORATORY FOAM EFFORTS

LA--UR--86-1916

DE86 012390

AUTHOR(S) JOEL M. WILLIAMS, MST-7
MARK H. WILKERSON, MST-7
DEBRA A. WROBLESKI, MST-7

SUBMITTED TO PROCEEDINGS OF THE SIXTH ADVANCED MATERIALS WORKSHOP
LAWRENCE LIVERMORE NATIONAL LABORATORY, LIVERMORE, CALIFORNIA
JUNE 3-5, 1986

DISCLAIMER

This report was prepared as an account of work sponsored by an agency of the United States Government. Neither the United States Government nor any agency thereof, nor any of their employees, makes any warranty, express or implied, or assumes any legal liability or responsibility for the accuracy, completeness, or usefulness of any information, apparatus, product, or process disclosed, or represents that its use would not infringe privately owned rights. Reference herein to any specific commercial product, process, or service by trade name, trademark, manufacturer, or otherwise does not necessarily constitute or imply its endorsement, recommendation, or favoring by the United States Government or any agency thereof. The views and opinions of authors expressed herein do not necessarily state or reflect those of the United States Government or any agency thereof.

By acceptance of this article the publisher recognizes that the U S Government retains a nonexclusive royalty-free license to publish or reproduce the published form of this contribution or to allow others to do so for U S Government purposes

The Los Alamos National Laboratory requests that the publisher identify this article as work performed under the auspices of the U S Department of Energy

Los Alamos Los Alamos National Laboratory
Los Alamos, New Mexico 87545

POTPOURRI OF LOS ALAMOS NATIONAL LABORATORY FOAM EFFORTS

by

Joel M. Williams, Mark H. Wilkerson, and Debra A. Wrobleski
Materials Science & Technology Division
Los Alamos National Laboratory
P.O. Box 1663
Los Alamos, NM 87545

ABSTRACT

This presentation provides an update on microcellular foam research efforts at Los Alamos. Topics include the influence of pressure on the phase separation of poly(4-methyl-1-pentene) from organic solution, a new concept of phase diagrams, physical testing of foams, and recent emulsion polymerization results.

Effect of Pressure on The Formation of Foam From PMP/Cumene

Cumene has produced the finest cell structure to date with PMP [poly(4-methyl-1-pentene)]. We have made a series of foams in which the pressure at the time of phase separation has been varied. The pressure range studied was 0.2 atm (3 psi) to 375 atm (5,500 psi). SEMs of some of the foams produced are presented in Fig. 1. The 0.2 atm sample had numerous cracks in the bulk material but the microstructure is not significantly poorer than the atmospheric samples. The sample produced in the sealed test tube is better than the atmospheric one as previously observed for diisopropylbenzene/PMP mixes. Increased pressure obviously reduces the cell sizes, but even at 375 atm (5,500 psi), substantially more reduction is needed if 1 μm cell size is to be achieved.

An attempt to induce rapid phase separation involved sudden release of the pressure at a temperature below the atmospheric phase separation temperature. The structure is seen in Fig. 1. These particular conditions did not give the desired result. Pressure releases at higher and lower temperatures are planned.

3-D Polymer-Solvent Phase Diagrams

As a result of our studies of the separation of PMP from various solvent solutions, we have concluded that the conventional 2-D phase diagrams do not predict the proper system behavior. Our reason is related to the fact that cloud point observations (T_c versus Θ_p) probably do not represent the actual separating phases. We believe that the observed 2-D cloud point diagrams are actually compressed 3-D representations as illustrated in Fig. 2. The problem originates with the difference in mobility of the solvent versus that of the polymer. Standard 2-D representations make an assumption that the two components have the same ability to rearrange, i.e. that the system is kinetically fluid or that each component is as fluid as any other. Such is not the case with a polymer-solvent system. Plasticization of a polymer is represented by the shaded surface in Fig. 3. Phase separation is visualized as $\emptyset_2' \rightarrow (\emptyset_2') +$ solvent. The separating phases are not defined by the normal binodal curve $\emptyset_2' \rightarrow \emptyset_2''$, but $\emptyset_2' \rightarrow \emptyset_2'' \rightarrow (\emptyset_2'')$, etc... as shown in Fig. 4. The 3-D representation allows us to explain the production of foams by thermally induced phase separation. Rapid cooling causes the polymer to separate under conditions in the front of the phase diagram rectangular prism (Fig. 3). Slower cooling allows the system to move towards the back. A change in mechanism around the peak in the binodal curve is,

thus not predicted. This is fortunate, since no change is observed although the 2-D representation predicts a change.

Compressive Strength of PMP Foams

Several years ago, we presented data for the compressive strengths of PMP foams made by two processes. These results with the correct strength units are given in Fig. 5. These data fit the empirical equation given in Fig. 5. We have now extended our analysis of the compressive strength of foams to account for non-supporting material in the foam, and for a change in the efficiency of the supporting material. The compressive strength of a foam is thus given by

$$\frac{E}{E_s} = \phi^2 \left[\frac{\rho - \rho^* \left(1 - \frac{\rho}{\rho_s}\right)}{\rho_s} \right]^2$$

where the subscripts refer to full density polymer, E is the elastic modulus, ϕ is the strength of the supporting material relative to the full density polymer, ρ is the density, and ρ^* is the density of the unsupporting material (a in Fig. 5). The fit of this equation to the observed data is given in Fig. 6, using $\phi = 1$. The straight line predicted by the equation in Fig. 6 represents the current literature thinking. The new equation fits the data and provides for a better understanding of the influence of foam structure on compressive strength. The amount of supportive and non-supporting material is important. So is the way the supporting material is configured (pore structure, ladder or honeycomb arrangements, etc.). So is the change in the strength of the polymer walls as probably occurs during the production of blown foams.

Applied to aerogel the equation predicts (assuming $\phi = 1$) that 80+% of the SiO_2 material is nonsupporting. This fits well with SEM of this material.

PS Foams From Polymerized Emulsions

PS foams can be obtained by polymerizing styrene dispersed in water as a water-in-oil emulsion [Unilever Pat. EP 60,138, (1982)]. Standard stirring techniques used to prepare the emulsion introduce air. We have devised an airless mixer (Fig. 7) that eliminates this problem. Flawless (no holes greater than 20 μm) PS/DVB foam cylinders have been prepared.

During our studies of the emulsion systems we attempted to reduce the density of the ultimate foam by diluting the PS/DVB oil component with nonpolymerizing dodecane. What resulted was not a significant reduction in density, but a surprising foam structure and great insight into the mechanics of emulsions. The influence of adding dodecane is seen in Figs. 8-10: the foam in Fig. 8 had no dodecane in the emulsion; that in Fig. 9 had some; and that in Fig. 10 had a lot. Note the delicate nature of the foam in Fig. 9. (3-D inspection can be made by crossing ones eyes so that the two pictures form three and then looking at the center one.) An explanation will be published elsewhere. These foams were prepared by the stirring method.

EFFECT OF PRESSURE ON PMP/CUMENE PHASE SEPARATION

3 PSI

11 PSI

Sealed Tube

1750 PSI

5500 PSI

6200 → 11 PSI
at 73-75°C

(Pressures at 70 C, 5% PMP)

FIGURE 1

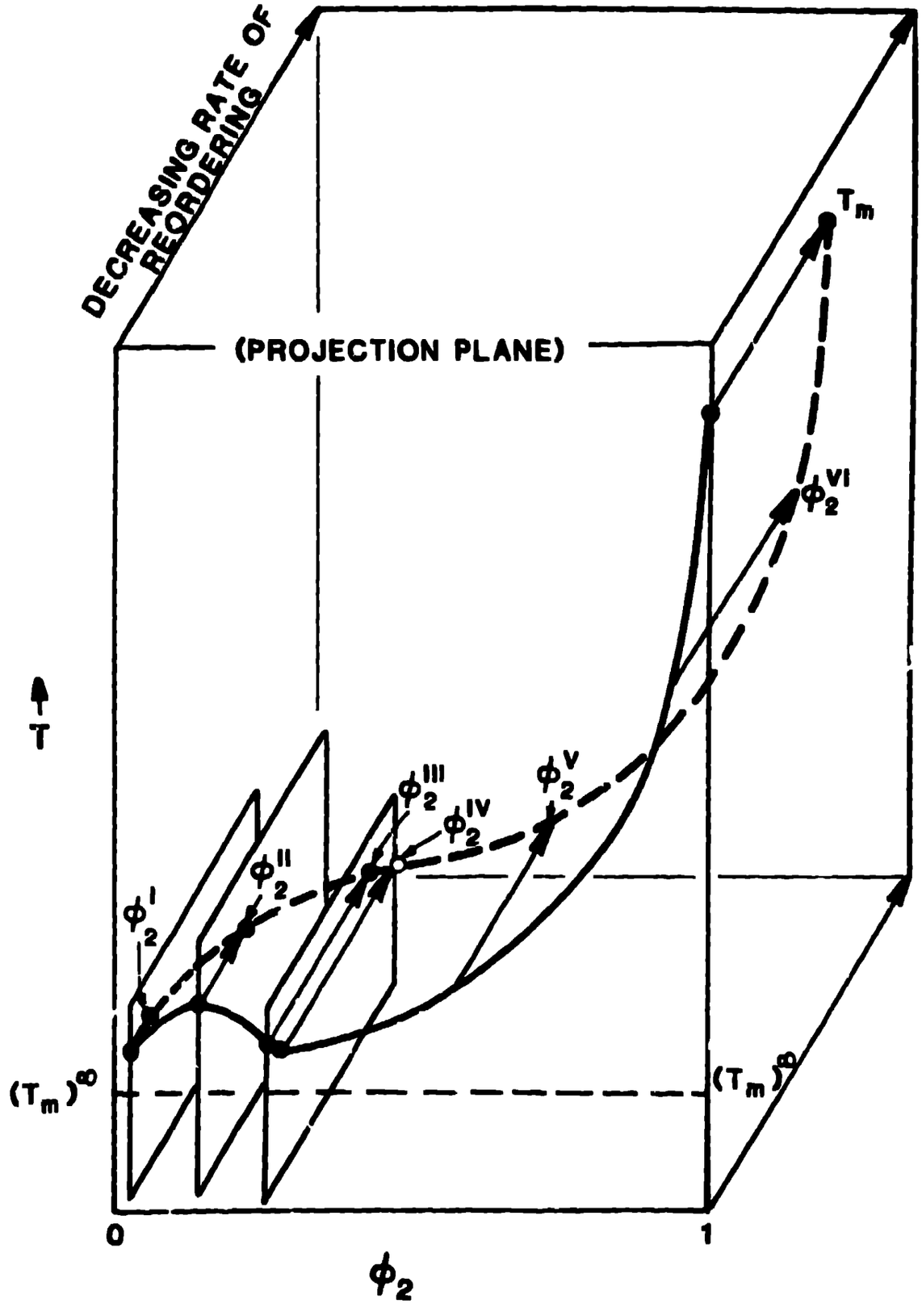
DECREASING RATE OF REORDERING
(PROJECTION PLANE)
T_m
ϕ_2^{VI}
T
ϕ_2^{III}
ϕ_2^{V}
ϕ_2^{IV}
ϕ_2^{II}
ϕ_2^{I}
$(T_m)^{\infty}$
$(T_m)^{\infty}$
0
1
ϕ_2

FIGURE 2

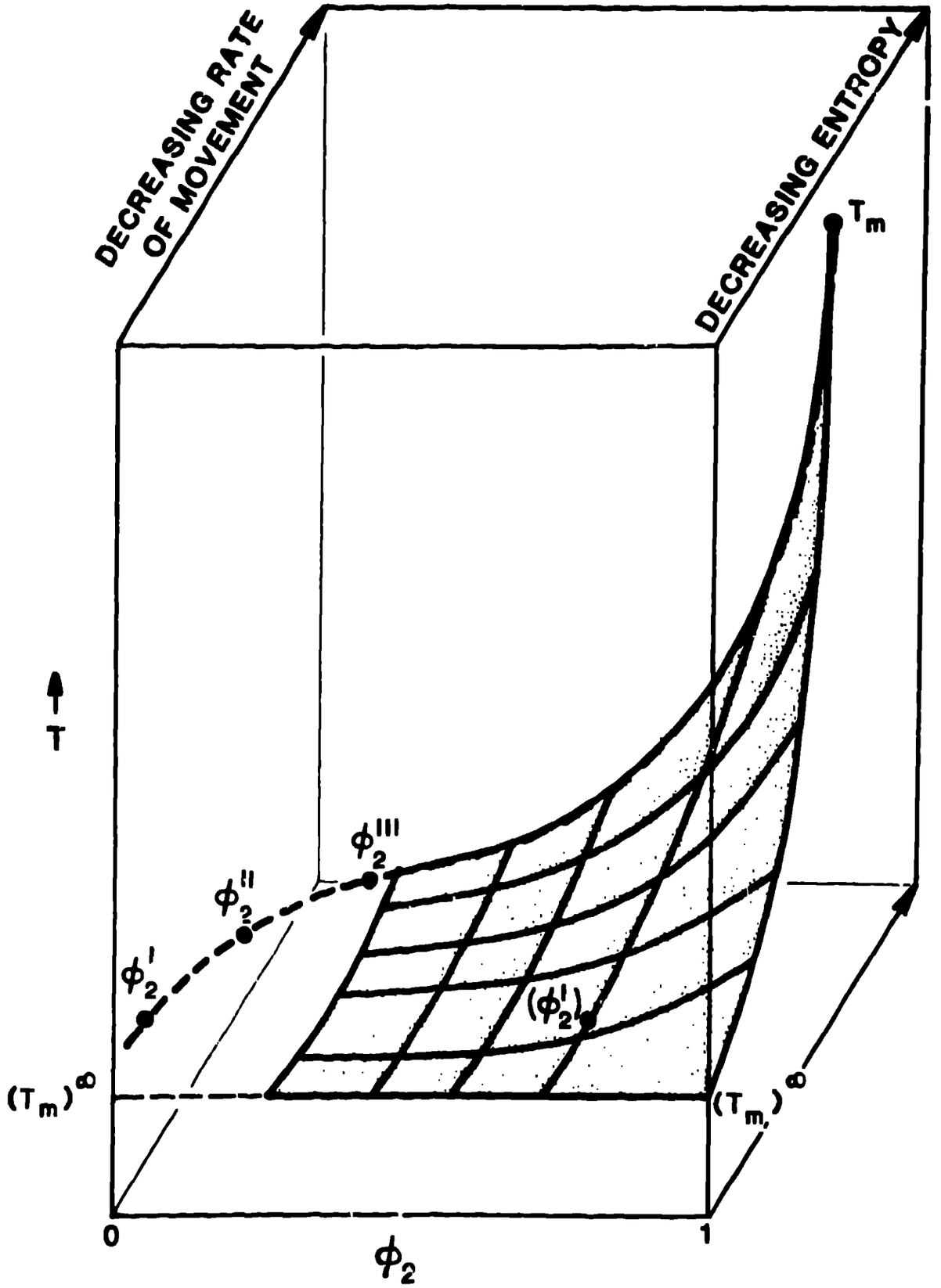
DECREASING RATE OF MOVEMENT
DECREASING ENTROPY
T_m
T
ϕ_2^{III}
ϕ_2^{II}
ϕ_2^{I}
(ϕ_2^{I})
$(T_m)^{\infty}$
$(T_m)^{\infty}$
0
1
ϕ_2

FIGURE 3

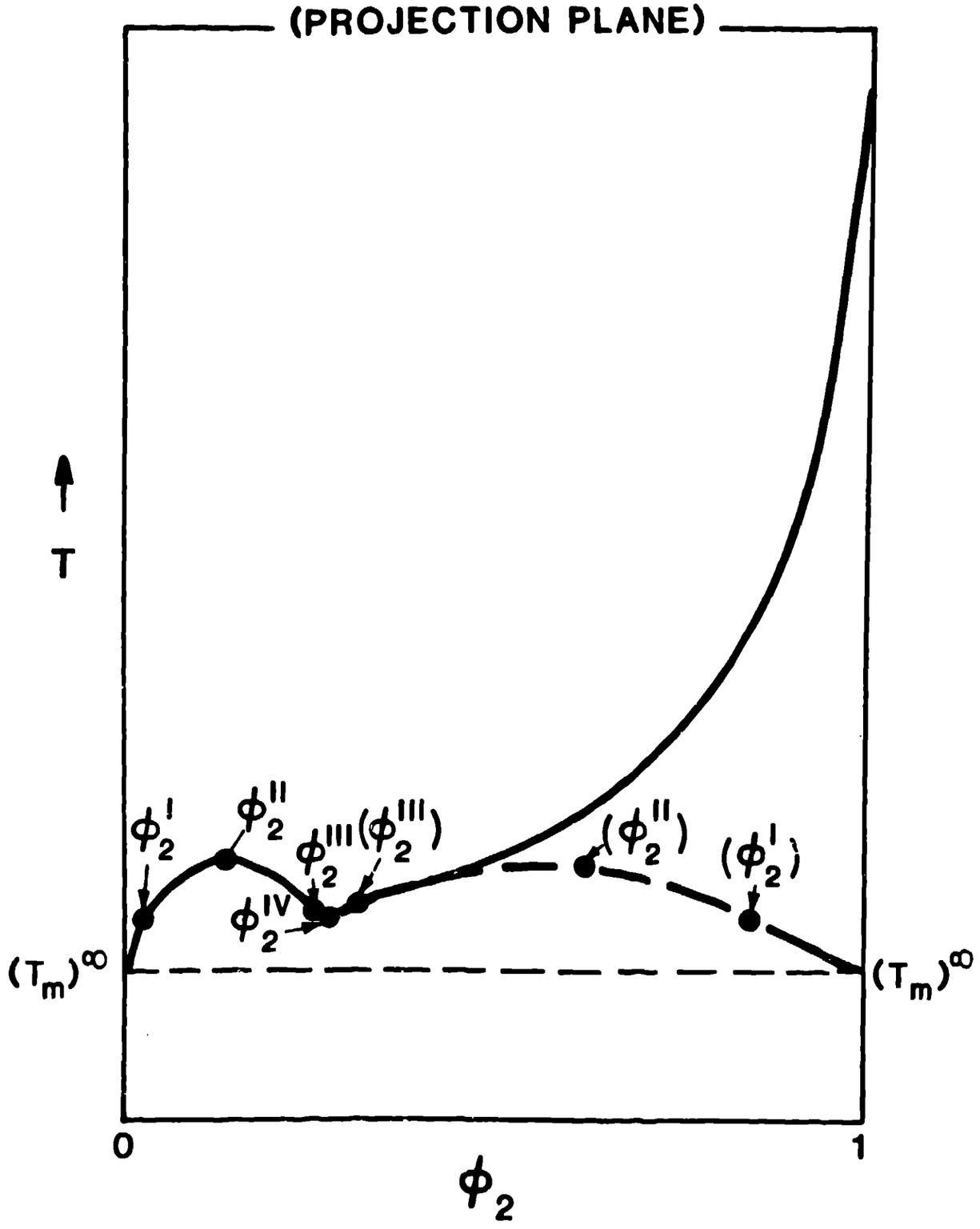
(PROJECTION PLANE)
T
ϕ_2^I
ϕ_2^{II}
ϕ_2^{III} (ϕ_2^{III})
ϕ_2^{IV}
(ϕ_2^{II})
(ϕ_2^I)
$(T_m)^\infty$
$(T_m)^\infty$
0
1
ϕ_2

FIGURE 4

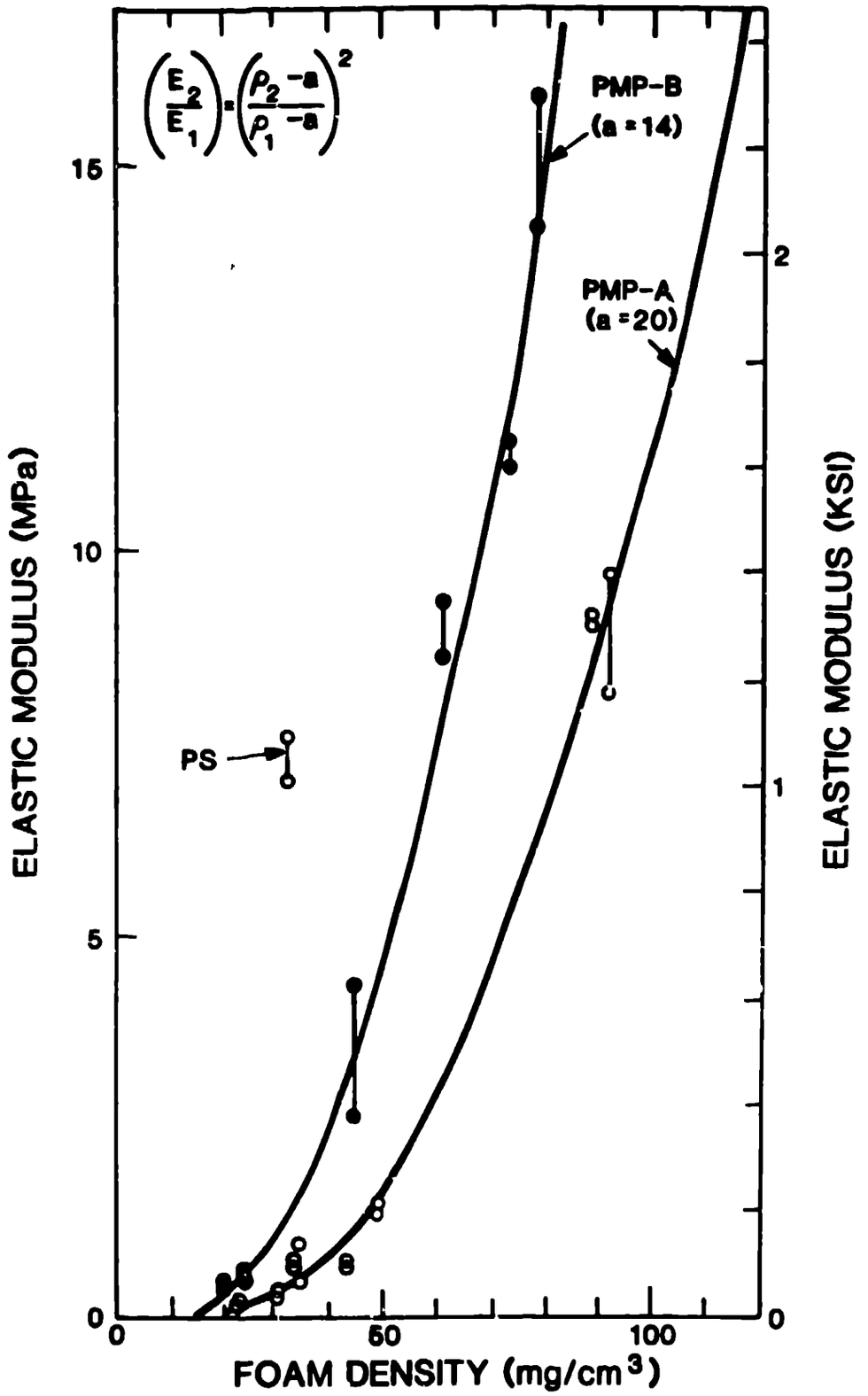
$\left(\frac{E_2}{E_1}\right)=\left(\frac{\rho_2-a}{\rho_1-a}\right)^2$
PMP-B
(a = 14)
PMP-A
(a = 20)
PS
ELASTIC MODULUS (MPa)
ELASTIC MODULUS (KSI)
FOAM DENSITY (mg/cm^3)
0
5
10
15
0
50
100
0
1
2

FIGURE 5

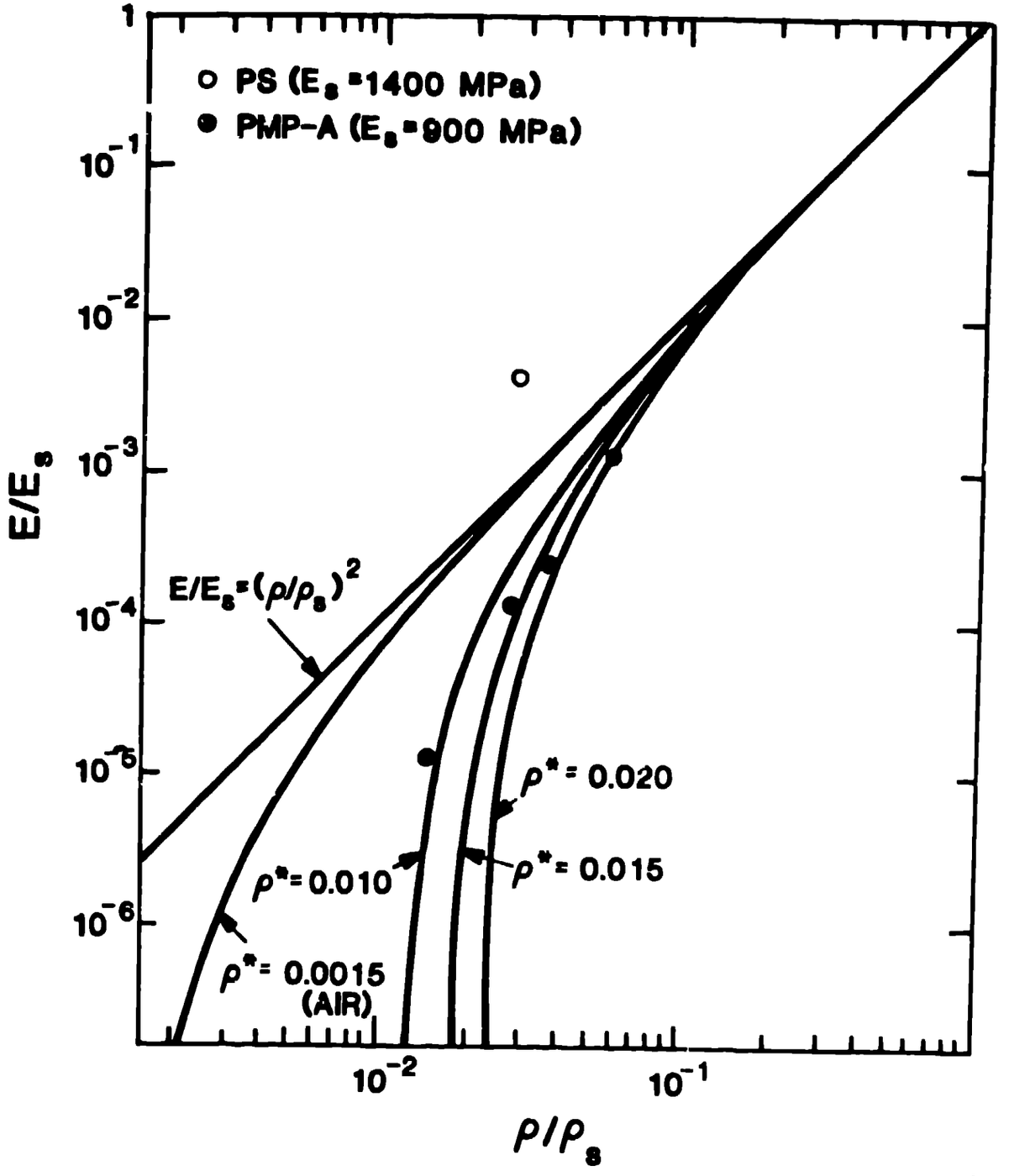
1
10^{-1}
10^{-2}
10^{-3}
10^{-4}
10^{-5}
10^{-6}
E/E_s
PS (E_s=1400 MPa)
PMP-A (E_s=900 MPa)
$E/E_s=(\rho/\rho_s)^2$
ρ^*= 0.020
ρ^*= 0.015
ρ^*= 0.010
ρ^*= 0.0015
(AIR)
10^{-2}
10^{-1}
ρ/ρ_s

FIGURE 6

FIGURE 7

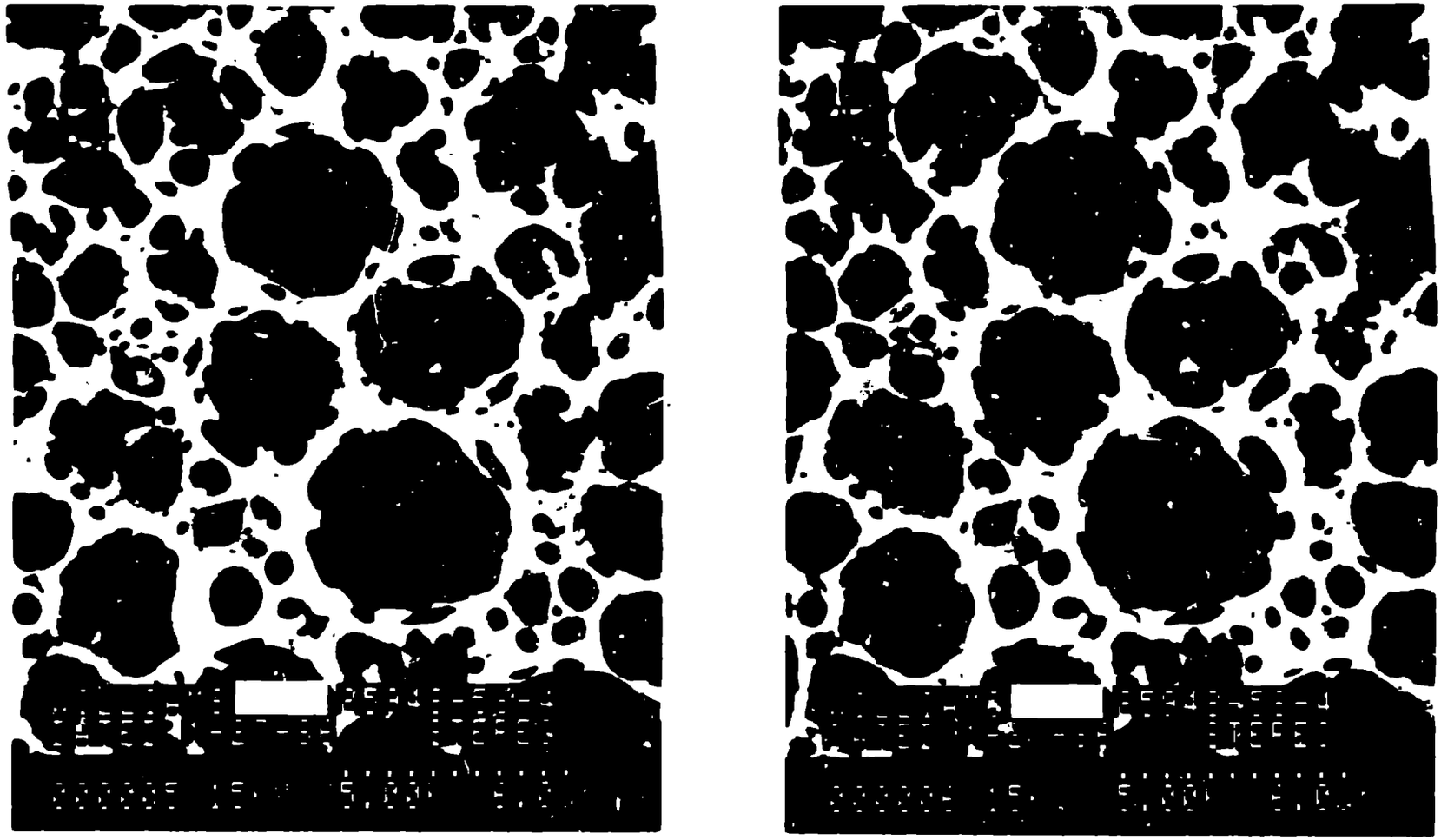

FIGURE 8

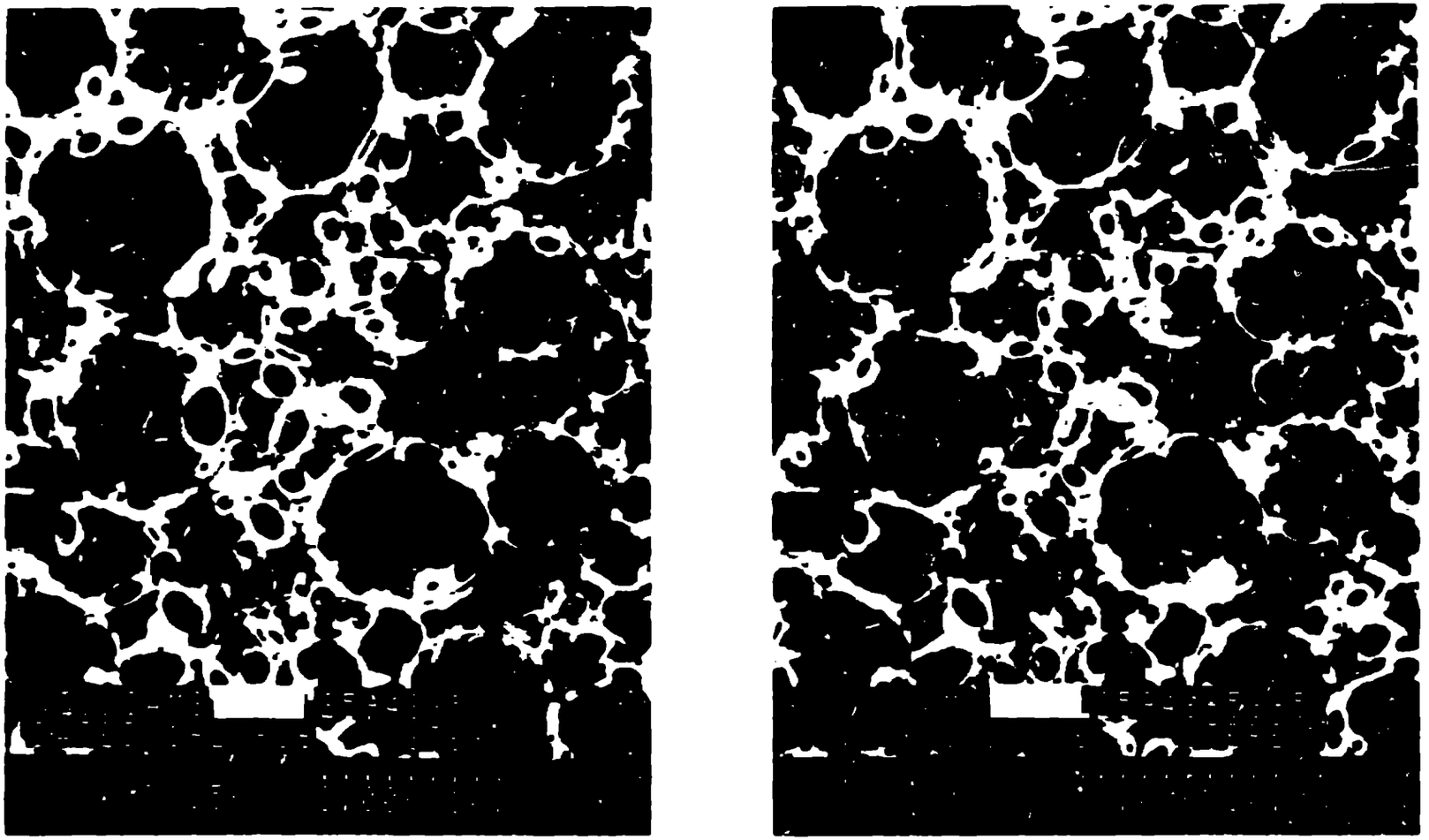

FIGURE 9

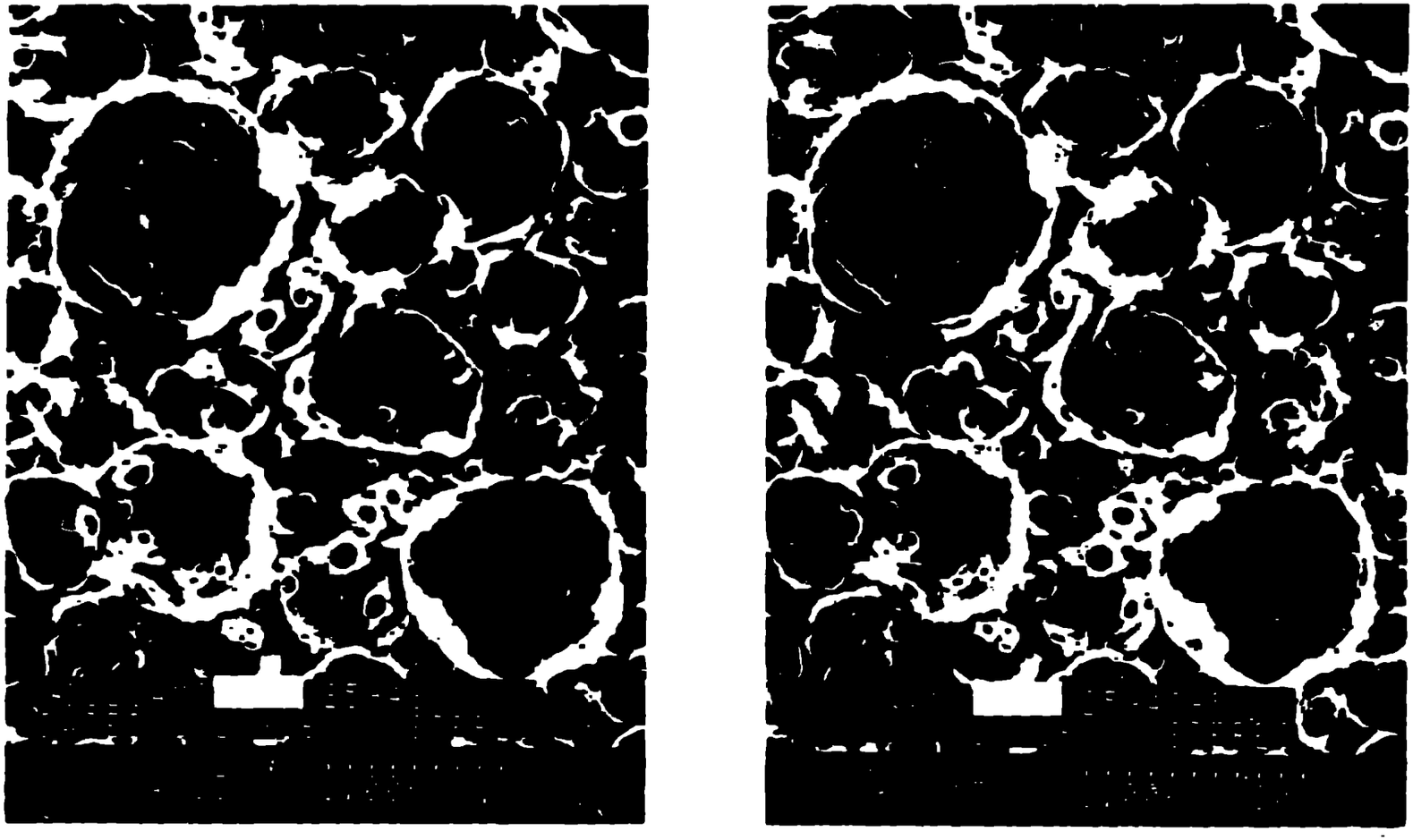

FIGURE 10